Heparanase inhibitor OGT 2115 induces prostate cancer cell apoptosis via the downregulation of MCL-1

XIN LI[1*], SHUAI-JUN XU[2*], BIN JIN[2*], HONG-SHENG LU[3], SHAN-KUN ZHAO[1], XIAO-FEI DING[4], LING-LONG XU[5], HAI-JUN LI[6], SHUANG-CHUN LIU[7], JIE CHEN[4] and GUANG CHEN[4,5]

[1]Department of Urology, Taizhou Central Hospital (Taizhou University Hospital), Taizhou University, Taizhou, Zhejiang 318000; [2]Graduate School of Medicine, Hebei North University, Zhangjiakou, Hebei 075000; [3]Department of Pathology, Taizhou Central Hospital (Taizhou University Hospital); [4]Department of Pharmacology, Taizhou University; [5]Department of Hematology, Taizhou Central Hospital (Taizhou University Hospital); [6]Department of Neurology, Taizhou Second People's Hospital, Taizhou University; [7]Laboratory Department, Municipal Hospital Affiliated to Taizhou University, Taizhou, Zhejiang 318000, P.R. China

Received July 28, 2023; Accepted October 31, 2023

DOI: 10.3892/ol.2024.14217

Abstract. Heparanase (HPSE), an endo-β-D-glucuronidase, cleaves heparan sulfate and serves an important role in the tumor microenvironment and thus in tumorigenesis. HPSE is known to promote tumor cell evasion of apoptosis. However, the underlying mechanism of this requires further study. In the present study, the results demonstrated that myeloid cell leukemia-1 (MCL-1), an antiapoptotic protein, and HPSE were upregulated in prostate cancer tissues compared with adjacent normal tissues. In addition, the HPSE inhibitor, OGT 2115, inhibited PC-3 and DU-145 prostate cancer cell viability in a dose-dependent manner, with IC_{50} values of 20.2 and 97.2 μM, respectively. Furthermore, annexin V/PI double-staining assays demonstrated that OGT 2115 induced apoptosis in prostate cancer cells. OGT 2115 treatment markedly decreased MCL-1 protein expression levels, whereas RNA interference-mediated downregulation of MCL-1 and OGT 2115 drug treatment synergistically induced apoptosis in PC-3 and DU-145 cells. *In vivo*, OGT 2115 40 mg/kg (ig) significantly inhibited PC-3 cell xenograft growth in nude mice and increased the positive TUNEL staining rate of xenograft tissues. It was therefore hypothesized that MCL-1 was an important signaling molecule in OGT 2115-induced apoptosis. The results of the present study also demonstrated that the proteasome inhibitor, MG-132, markedly inhibited the downregulation of MCL-1 protein expression levels induced by OGT 2115. However, the protein synthesis inhibitor, cycloheximide, did not affect the role of OGT 2115 in regulating MCL-1. In summary, the results of the present study demonstrated that the proapoptotic activity of OGT 2115 was achieved by downregulating MCL-1.

Correspondence to: Mrs. Jie Chen or Dr Guang Chen, Department of Pharmacology, Taizhou University, 1139 Shi-Fu Avenue, Taizhou, Zhejiang 318000, P.R. China
E-mail: jchen2012@tzc.edu.cn
E-mail: gchen@tzc.edu.cn

*Contributed equally

Key words: heparanase, prostate cancer, apoptosis, MCL-1

Introduction

Prostate cancer is a malignancy that seriously threatens men's health and ranks second in the cancer incidence rate in men worldwide. The incidence of prostate cancer in China is increasing, the age-standardized incidence rate of prostate cancer was 17.3 individuals in 100,000 in 2019 in China, which was a 95.2% rise compared with 1990 (1,2). Surgery and radiotherapy are the standard treatments for early-stage prostate cancer. However, patients with advanced or metastatic prostate cancer require androgen deprivation therapy, which includes surgery or medical castration (3). Prostate cancer commonly leads to bone metastasis, which is the main cause of morbidity and mortality in patients (4,5). Therefore, it is necessary to investigate the molecular mechanism of prostate cancer metastasis and develop novel therapeutic approaches to inhibit the invasion and metastasis of prostate cancer cells.

Heparanase (HPSE) is a β-D-endoglycosidase (also referred to as an endo-β-D-glucuronidase) that degrades the heparan sulfate (HS) side chain of HS proteoglycans (HSPGs) (6). HSPGs are a dynamic structural component that are widely distributed on the cell surface and in the extracellular matrix (ECM) (7). Active HPSE is associated with various diseases, including cancer (8). Furthermore, HPSE is upregulated in almost all malignant tumor tissues (9) and is commonly associated with the tumor microenvironment (10).

Myeloid cell leukemia-1 (MCL-1) is an antiapoptotic member of the Bcl-2 family (11). MCL-1 is mainly located in the cytoplasm and mitochondria and interacts with proapoptotic proteins, including phorbol-12-myristate-13-acetate-induced protein 1, Bcl-2-like protein 11, Bcl-2 homologous antagonist/killer (BAK) and Bax, to exert antiapoptotic effects (12).

The stability and functional activity of MCL-1 are regulated via phosphorylation modifications (13). Moreover, MCL-1 is upregulated in cancer following genetic, epigenetic or signaling pathway alterations (14). Upregulation of MCL-1 can inhibit tumor cell apoptosis and improve tumor cell resistance to chemotherapy drugs (15). Furthermore, MCL-1 is highly expressed in prostate cancer, particularly in metastatic prostate cancer, and therefore inhibiting MCL-1 promotes prostate cancer cell apoptosis and improves the chemotherapy sensitivity of prostate cancer cells (16).

In the present study, the expression profiles of HPSE and its correlation with MCL-1 in prostate cancer were investigated using The Cancer Genome Atlas (TCGA) database analysis. The roles of HPSE in prostate cancer were further determined using prostate cancer cell line models *in vitro* and a xenograft model *in vivo*. The mechanism of HPSE regulating MCL-1 was also explored using HPSE inhibitor treatment and western blotting, which may help to understand its role in prostate cancer progression.

Materials and methods

Cell culture and treatments. The human prostate carcinoma PC-3 and DU-145 cell lines were purchased from The Cell Bank of Type Culture Collection of The Chinese Academy of Sciences. PC-3 cells were cultured in F12 medium (containing 300 mg/l L-glutamine and 1.5 g/l $NaHCO_3$; Thermo Fisher Scientific, Inc.) supplemented with 10% FBS (Thermo Fisher Scientific, Inc.). DU-145 cells were maintained in DMEM (Thermo Fisher Scientific, Inc.) supplemented with 10% FBS. Both cell lines were cultured at 37˚C in a humidified incubator with 5% CO_2. The HSPE inhibitor, OGT 2115, MG-132 and cycloheximide (CHX) were purchased from MedChemExpress.

TCGA data analysis. The analysis of TCGA prostate adenocarcinoma data (17) was performed by using the UALCAN (https://ualcan.path.uab.edu/analysis.html) platform according to previously published protocols (18,19). $P<0.01$ and log2 |Fold Change| >1 were considered as the significant thresholds. In the survival analysis, the high and low expression groups were determined using the median expression level as the cut-off. The Pearson correlation coefficient between HPSE and MCL-1 was calculated using the GEPIA (http://gepia.cancer-pku.cn/index.html) platform.

Patients. A total of six prostate cancer tissue samples (including the adjacent normal tissue) were collected from Taizhou Central Hospital (Taizhou, China), and written consent was obtained from all patients for the use of their tissues in the present study. Patients who were diagnosed with advanced prostate cancer from May 2021 to Jan 2023 were included in the present study. The inclusion criteria were as follows: i) Patients with stage IV-V prostate cancer; and ii) patients with a single primary tumor or patients who had only one prior tumor. The exclusion criteria were as follows: i) Patients whose prior cancer was prostate cancer; ii) patients with incomplete follow-up data; iii) patients with only death certificates or autopsy records; and iv) patients whose time of malignancy diagnosis was not known. The baseline patient demographics and clinical characteristics are shown in Table I. Gleason score was determined by following the 'Gleason Grading of Prostatic Carcinoma: Definition of Grading Patterns and Proposal for a New Grading System' guidelines (20). The present study was performed in accordance with the ethical standards of The Taizhou Central Hospital Research Committee and The Declaration of Helsinki, or comparable ethical standards. The study was approved by The Medical Ethics Committee of Taizhou Central Hospital (approval no. 2021-SC-076).

Immunohistochemistry. Each patient and mouse tissue sample was treated according to the following protocol: The 30-μm free-floating sections were deparaffinized, antigen retrieval was performed, and the endogenous peroxidase activity was removed. Briefly, the samples were rehydrated using xylene and graded concentrations of ethanol (100% ethanol for 5 min three times, 95% ethanol for 5 min once and 80% ethanol for 5 min once), incubated in sodium citrate (10 mmol/l, pH 6.0) at 95˚C for 10 min and then cooled down to room temperature, followed with blocking for endogenous peroxidase using 3% hydrogen peroxide (Thermo Fisher Scientific, Inc.) for 30 min at room temperature. Sections were permeabilized with 0.1% Triton and blocked in 10% goat serum (Beyotime Institute of Biotechnology) for 30 min at room temperature. The tissue sections were then incubated with the relevant primary antibody overnight at 4˚C. The HPSE antibody (1:200; cat. no. 24529-1-AP) was purchased from Proteintech Group, Inc. and the MCL-1 (1:200; cat. no. 94296) and Ki-67 (1:200; cat. no. 12202) antibodies were purchased from Cell Signaling Technology, Inc. Following the primary incubation, sections were washed using PBS and then incubated with a goat anti-rabbit secondary antibody conjugated with HRP (cat. no. 554021; 1:200; BD Pharmingen; BD Biosciences) for 30 min at room temperature. Then, DAB staining and hematoxylin counter-staining were performed for 2 min at room temperature. Images of the sections were collected using a light microscope (Olympus BX-51).

Cell viability. Cell viability was assessed using the MTT assay. PC-3 and DU-145 cells ($3x10^3$ cells/well) were seeded into 96-well cell culture plates and treated with OGT 2115 at different concentrations (300, 100, 33.33, 11.11, 3.67 and 1.22 μM) for 72 h at 37˚C. 0.3% DMSO was set as control solvent. Subsequently, 20 μl MTT reagent (5 mg/ml) was added to each well and incubated at 37˚C for 4 h. The MTT crystals were dissolved using DMSO for 10 min at room temperature with gentle shaking, and the absorbance at 492 nm was recorded.

Reverse transcription-quantitative PCR (RT-qPCR). Total RNA from cells following treatment (PC-3 cells were treated with OGT 2115 at concentrations of 0, 10, 20 and 40 μM, whereas DU-145 cells were treated with concentrations of 0, 25, 50 and 100 μM, both for 24 h) was extracted using RNAiso reagent (Takara Biotechnology Co., Ltd.) and complementary (c)DNA was synthesized using an RT kit (Takara Biotechnology Co., Ltd.) according to the manufacturer's protocol. Subsequently, the cDNA was amplified using SYBR (Takara Biotechnology Co., Ltd.) in a PCR Thermal Cycler Dice Real-Time System according to the manufacturer's protocol. mRNA expression

Table I. Baseline patient demographics and clinical characteristics.

Patient no.	Age, years	Gleason score	History of anticancer drug treatment
1	61	6	No
2	73	7	No
3	71	6	No
4	62	7	No
5	60	6	No
6	71	7	No

levels were analyzed using the $2^{-\Delta\Delta Cq}$ method (21) and were normalized to the internal reference gene, GAPDH. The primers used for qPCR were as follows: GAPDH forward, 5'-GCACCGTCAAGGCTGAGAAC-3' and reverse, 5'-GCCTTCTCCATGGTGGTGAA-3'; and MCL-1 forward, 5'-GGGCAGGATTGTGACTCTCATT-3' and reverse, 5'-GATGCAGCTTTCTTGGTTTATGG-3'.

Western blotting. PC-3 cells were treated with OGT 2115 at concentrations of 0, 10, 20 and 40 μM, whereas DU-145 cells were treated with concentrations of 0, 25, 50 and 100 μM, both for 24 h. For the CHX and MG132 assays, CHX or MG132 was added to the culture medium at a final concentration of 35 μM or 10 mM, respectively. The CHX group was pretreated with OGT 2115 at concentrations of 0, 25, 50 and 100 μM for 18 h, and cell lysates were collected 6 h after CHX treatment. The MG-132 group was pretreated with OGT 2115 at concentrations of 0, 25, 50 and 100 μM for 22 h, and cell lysates were collected 2 h after MG-132 treatment. Total protein from cells following treatment was extracted using RIPA lysis buffer (Beyotime Institute of Biotechnology). Equivalent amounts of proteins (50 mg; quantified by BCA kit, Beyotime Institute of Biotechnology) were then separated via SDS-PAGE using a 10% gel and then transferred onto PVDF membranes (Bio-Rad Laboratories, Inc.). Subsequently, the membranes were blocked with non-fat dry milk (5%) in TBS with 0.1% Tween-20 for 2 h at room temperature, then probed with primary antibodies against HPSE (1:1,000; cat. no. 24529-1-AP; Proteintech Group, Inc), MCL-1 (1:1,000; cat. no. 94296; Cell Signaling Technology, Inc.) and tubulin (1:5,000; cat. no. sc-32293, Santa Cruz Biotechnology, Inc.) for 12 h at 4˚C. Following the primary antibody incubation, the membranes were incubated with an anti-rabbit IgG HRP-conjugated secondary antibody (1:5,000; cat. no. A0208; Beyotime Institute of Biotechnology) for 2 h at room temperature. The separated proteins were detected using an enhanced chemiluminescence kit (Beyotime Institute of Biotechnology). Tubulin was used as the loading control. The blots were scanned and semi-quantified using an Image Quant LAS 4000 Min. (GE Healthcare).

Small interfering (si)RNA transfection. A synthetic siRNA targeting MCL-1 (si-MCL-1; 5'-GUGCCUUUGUGGCUAAACATT-3') was purchased from Shanghai GenePharma Co., Ltd. Scrambled siRNA (5'-UUCUCCGAACGUGUCACGUTT-3') was used as a negative control (NC). When the cell density reached 60-70%, PC-3 and DU-145 cells were transfected with siRNA using Lipofectamine® 2000 (Invitrogen; Thermo Fisher Scientific, Inc.) according to the manufacturer's protocol with a final siRNA concentration of 100 nM.

Apoptosis determination assay. PC-3 cells were treated with OGT 2115 at concentrations of 0, 10, 20 and 40 μM, whereas DU-145 cells were treated with concentrations of 0, 25, 50 and 100 μM. Following treatment with OGT 2115, the cells were cultured for 24 h and apoptosis detected via flow cytometry. For this, PC-3 and DU-145 cells were digested using trypsin for 2 min at 37˚C, washed with PBS and resuspended in 100 μl 1X annexin V binding buffer containing 5 μl annexin V-FITC and 10 μl PI (Beyotime Institute of Biotechnology). Cells were then incubated for 15 min at room temperature in the dark. The percentage of PI-positive annexin V-FITC-positive/negative (PI^+/AV^- plus PI^+/AV^+) and PI-negative (PI^-)/AV^+ cells were quantified using flow cytometry (CytoFlex S; Beckman Coulter, Inc.), and Kaluza Analysis software version 1.2 (Beckman Coulter, Inc.) was used for subsequent analysis.

Xenograft assay. PC-3 cells ($2x10^6$ cells/200 μl) were inoculated subcutaneously into the right side of male BALB/c nude mice (age, 4-5 weeks; Beijing Vital River Laboratory Animal Technology Co., Ltd.). The mice were housed in sterile cages under laminar airflow hoods at 20˚C, in a specific pathogen-free environment, under a 12-h light/dark cycle and provided with autoclaved chow and water *ad libitum*. Animal health and behavior were monitored every day. Nude mice were divided into the following two groups: i) Vehicle control (4% ethanol, 5% PEG 400 and 5% Tween 80) group, n=7; and ii) OGT 2115 treatment group, n=6 (gavage; 40 mg/kg; once daily). When the tumors reached 30-40 mm^3 the mice were administered saline or OGT 2115 via gavage daily for 35 days. Vernier calipers were used to measure the length and width of the xenografts twice a week. The tumor volume was calculated using the formula volume=($Width^2$ x length)/2. At the end of the experiment, the mice were anesthetized with isoflurane (4%) and O_2 gas at 300-500 ml/min using the R540 Mice and Rat Animal Anesthesia Machine (RWD Life Science Co., Ltd.) for 10 min prior to sacrifice via cervical dislocation. The humane endpoints followed to determine whether animals should be euthanized before the end of the study were body weight loss of >20% and a tumor volume of >1,500 mm^3. In the present study, no animals reached these humane endpoints during the 3-month experiment. Subsequently, the tumors were dissected and weighed. A part of the tumor tissue was fixed with 10% formalin for 24-48 h at room temperature for subsequent experiments, the rest were immediately frozen in liquid nitrogen for storage in the event of further experimentation.

All experimental procedures involving animals were performed in accordance with The National Institutes of Health Guide for the Care and Use of Laboratory Animals and the Guide for the Care and Use of Laboratory Animals in China (22). The present animal study was approved by The Medical Ethics Committee of Taizhou University Medical School (Taizhou, China; approval no. 2021-SX-015).

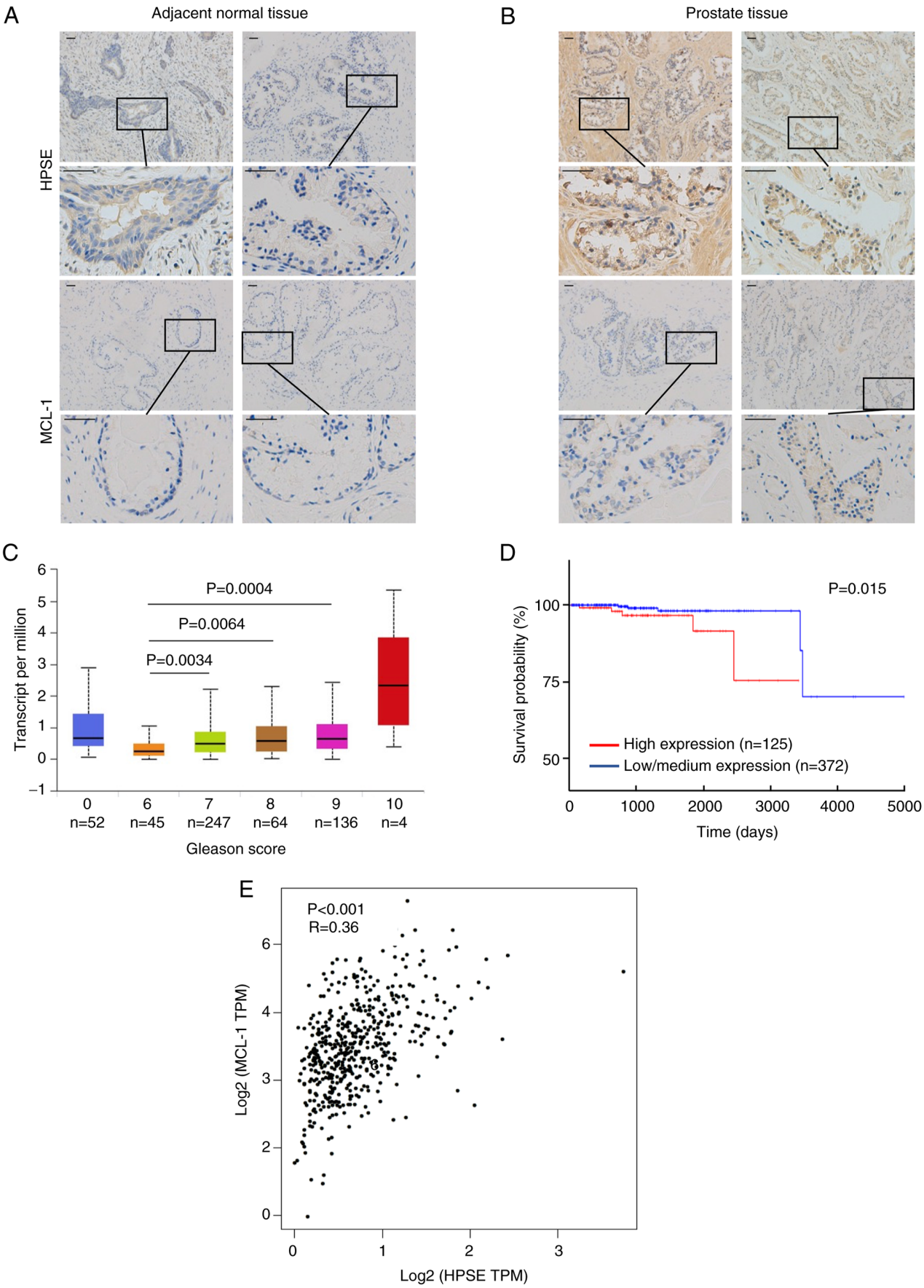

Figure 1. Expression profile of HPSE and MCL-1 in prostate cancer. Representative immunohistochemical staining of HPSE and MCL-1 proteins in human (A) adjacent normal prostate tissues and (B) prostate cancer tissues. Scale bar, 50 μm. (C) HPSE expression in prostate cancer tissues with different Gleason scores using the TCGA prostate adenocarcinoma dataset (17). (D) The correlation between HPSE expression levels and prognosis. (E) The relationship between HPSE and MCL-1 expression from TCGA prostate adenocarcinoma dataset (17). HPSE, heparanase; MCL-1, myeloid cell leukemia-1; TCGA, The Cancer Genome Atlas; TPM, transcripts per million.

TUNEL staining. To determine cell death, a TUNEL assay was conducted. Each sample was fixed using 4% Paraformaldehyde Fix Solution (cat. no. P0099: Beyotime Institute of Biotechnology) for 96 h at room temperature. The 5-μm free-floating sections were deparaffinized, antigen retrieval was performed, and the endogenous peroxidase activity was removed using 3% hydrogen peroxide (Thermo Fisher Scientific, Inc.) for 30 min at room temperature. Briefly, the samples were rehydrated using xylene and graded concentrations of ethanol (100% ethanol for 5 min three times, 95% ethanol for 5 min once and 80% ethanol for 5 min once), then immersed in 50 μl TUNEL reaction solution (cat. no. C1088; Beyotime Institute of Biotechnology), and then the slides were incubated for 60 min at 37˚C in a humid darkened chamber. 4',6-diamidino-2-phenylindole was subsequently applied to the slides for 5 min at room temperature in the dark to stain the nuclei, then mounted with Antifade Mounting Medium (cat no. P0128M; Beyotime Institute of Biotechnology), after which the slides were imaged with a fluorescence microscope, five fields of view observed by microscopy for each slide.

Statistical analysis. All statistical analyses were performed using GraphPad Prism 8.0 (Dotmatics). Statistical significance was assessed using an unpaired Student's t-test for two groups or a one-way ANOVA followed by Tukey's post hoc test for more than two groups. Data are presented as the mean ± SD. $P<0.05$ was considered to indicate a statistically significant difference.

Results

HPSE and MCL-1 are upregulated in prostate cancer tissues. To verify the abnormal expression of HPSE and MCL-1 in the development of prostate cancer, immunohistochemistry was performed on adjacent normal and prostate cancer tissues from patients. The results demonstrated that HPSE and MCL-1 were expressed in the cytoplasm and that the protein expression levels in the prostate cancer tissues were markedly higher compared with the adjacent normal tissues (Fig. 1A and B).

The expression profile of HPSE in prostate cancer tissues was also explored using a TCGA dataset (17). As shown in Fig. 1C, statistical tabulation analysis of the dataset demonstrated that HPSE expression was associated with the pathological tumor grade, and expression in Gleason score 7, 8 and 9 tumors was significantly higher than that in Gleason score 6 tumors ($P<0.001$). Moreover, the 5,000 days overall survival rate of patients with high expression of the HPSE gene was significantly lower than that of patients with Low/Medium expression ($P=0.015$; Fig. 1D).

A weak correlation between HPSE and MCL-1 expression was also determined ($r=0.36$, $P<0.01$; Fig. 1E) using the GEPIA (http://gepia.cancer-pku.cn/index.html). As HPSE expression is known to be associated with tumor progression (23) and MCL-1 is related to apoptosis (24), these results suggested that HPSE and MCL-1 may be involved in cell survival in prostate cancer cells.

OGT 2115 decreases cell viability. To further explore the role of HSPE in the progression of prostate cancer, PC-3 and DU-145 prostate cancer cells were treated with the HSPE inhibitor, OGT 2115 (Fig. 2A). The results demonstrated that, compared with cells treated with the control solvent, OGT 2115 treatment led to significantly decreased cell viability in both cell lines in a dose-dependent manner (Fig. 2B). The IC_{50} of OGT 2115 in PC-3 cells was 18.4 μM and the IC_{50} in DU-145 cells was 90.6 μM.

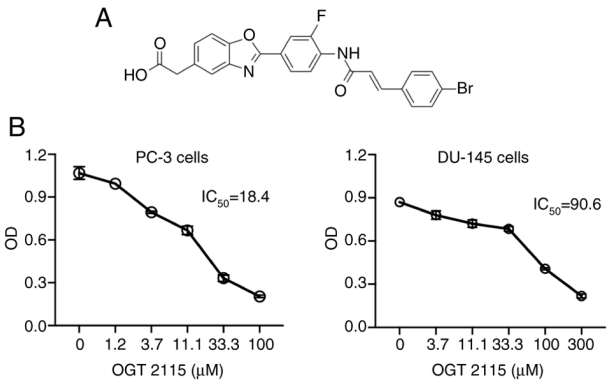

Figure 2. OGT 2115 decreases prostate cancer cell viability. (A) Molecular structure of the HPSE inhibitor, OGT 2115. (B) OGT 2115 inhibited PC-3 and DU-145 prostate cancer cell viability, which was detected using the MTT assay. HPSE, heparanase; OD, optical density.

OGT 2115 induces apoptosis and MCL-1 downregulation in prostate cancer cells. The effect of OGT 2115 on prostate cancer cell apoptosis was further determined using Annexin V-FITC/PI flow cytometry. PC-3 cells were treated with OGT 2115 at concentrations of 0, 10, 20 and 40 μM, whereas DU-145 cells were treated with concentrations of 0, 25, 50 and 100 μM. Following treatment with OGT 2115, the cells were cultured for 24 h and apoptosis detected via flow cytometry. In a dose-dependent manner, from the lowest OGT 2115 concentration to the highest, the apoptosis rates of the PC-3 cells were 4.21, 5.51, 8.12 and 9.50%, respectively, whereas the apoptosis rates of the DU-145 cells were 3.15, 11.02, 22.94 and 34.24%, respectively (Q1-LR in Fig. 3A).

In addition, OGT 2115 reduced MCL-1 protein expression levels in PC-3 and DU-145 cells but promoted the protein expression levels of caspase-3 and Bax (Fig. 3B and C).

OGT 2115 inhibits prostate cancer cell viability. To explore how the antitumor effect of OGT 2115 was associated with MCL-1 protein expression levels, RNA silencing experiments were conducted. MCL-1 protein expression levels were successfully downregulated using si-MCL-1 in PC-3 and DU-145 cells (Fig. 4A). Flow cytometry demonstrated that the PC-3 cell death rate was 6.25% in the si-NC group and 9.58% in the si-MCL-1 group (Fig. 4B). The cell death rate in the si-NC + OGT 2115 20 μM group was 19.4% and the cell death rate in the si-MCL-1 + OGT 2115 20 μM group was 22.64%. In DU-145 cells, the cell death rate was 7.24% in the si-NC group and 12.8% in the si-MCL-1 group (Fig. 4B). As shown in Fig. 4C, the cell death rate in the si-NC + OGT 2115 100 μM group was 22.68%, whereas the cell death rate of the si-MCL-1 + OGT 2115 100 μM group was 24.63%. These results support the suggestion that OGT 2115 inhibits prostate cancer cell viability.

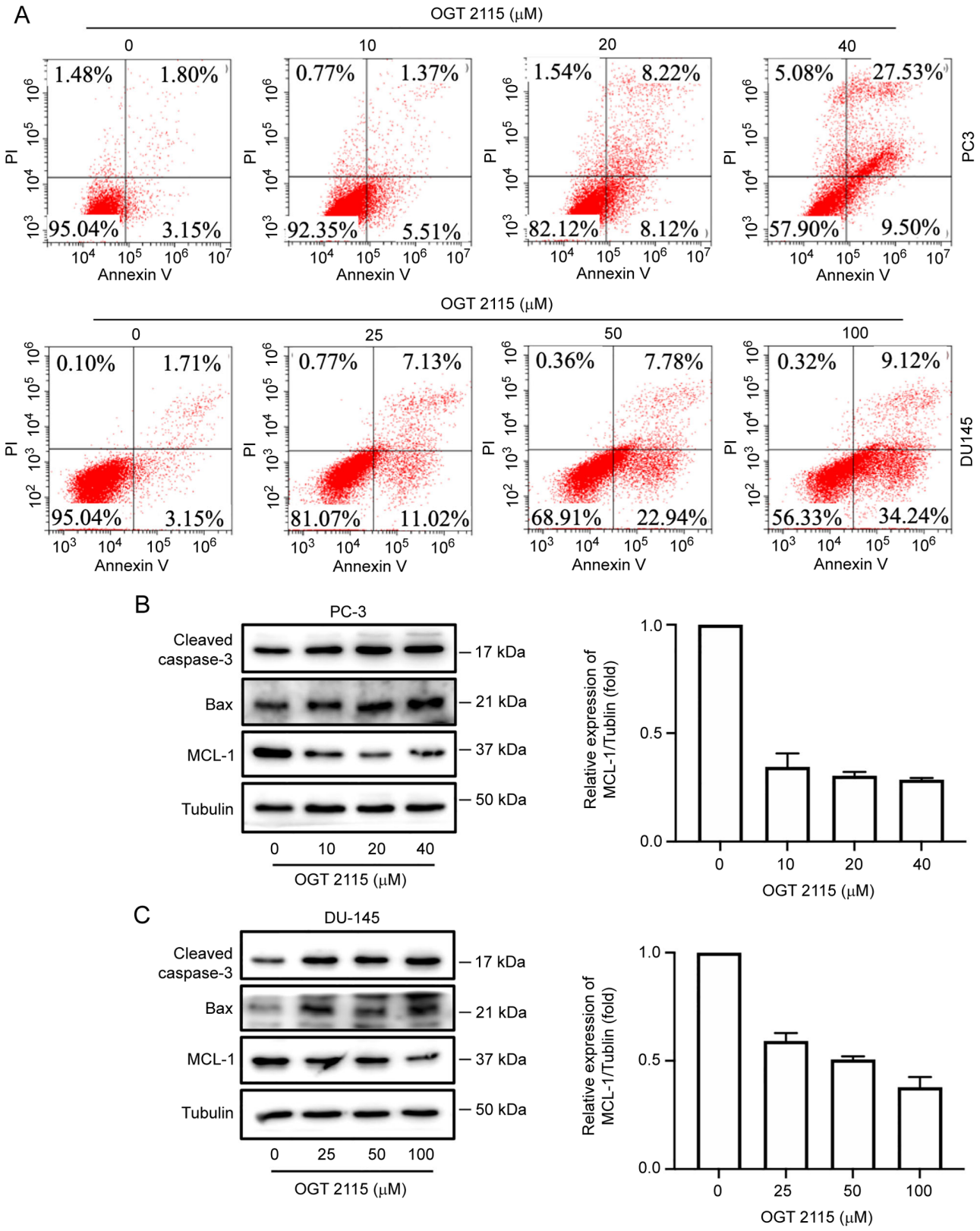

Figure 3. OGT 2115 induces PC-3 and DU-145 prostate cancer cell apoptosis. (A) Flow cytometry using annexin V (x-axis) and PI (y-axis) was conducted to determine the apoptosis rate in each experimental group. Protein expression levels of apoptosis-related proteins following OGT 2115 treatment in (B) PC-3 and (C) DU-145 cells were determined via western blotting. Tubulin was used as a loading control. MCL-1, myeloid cell leukemia-1.

OGT 2115 inhibits prostate cancer cell xenograft growth in nude mice. To further validate the role of OGT 2115 in prostate cancer, *in vivo* experiments were conducted. PC-3 cells were injected subcutaneously into the right side of nude mice. When the tumors reached 30-40 mm^3 the mice were administered saline or OGT 2115 via gavage daily for 35 days. The results demonstrated that tumor growth was significantly inhibited in the OGT 2115 group compared with the control group at

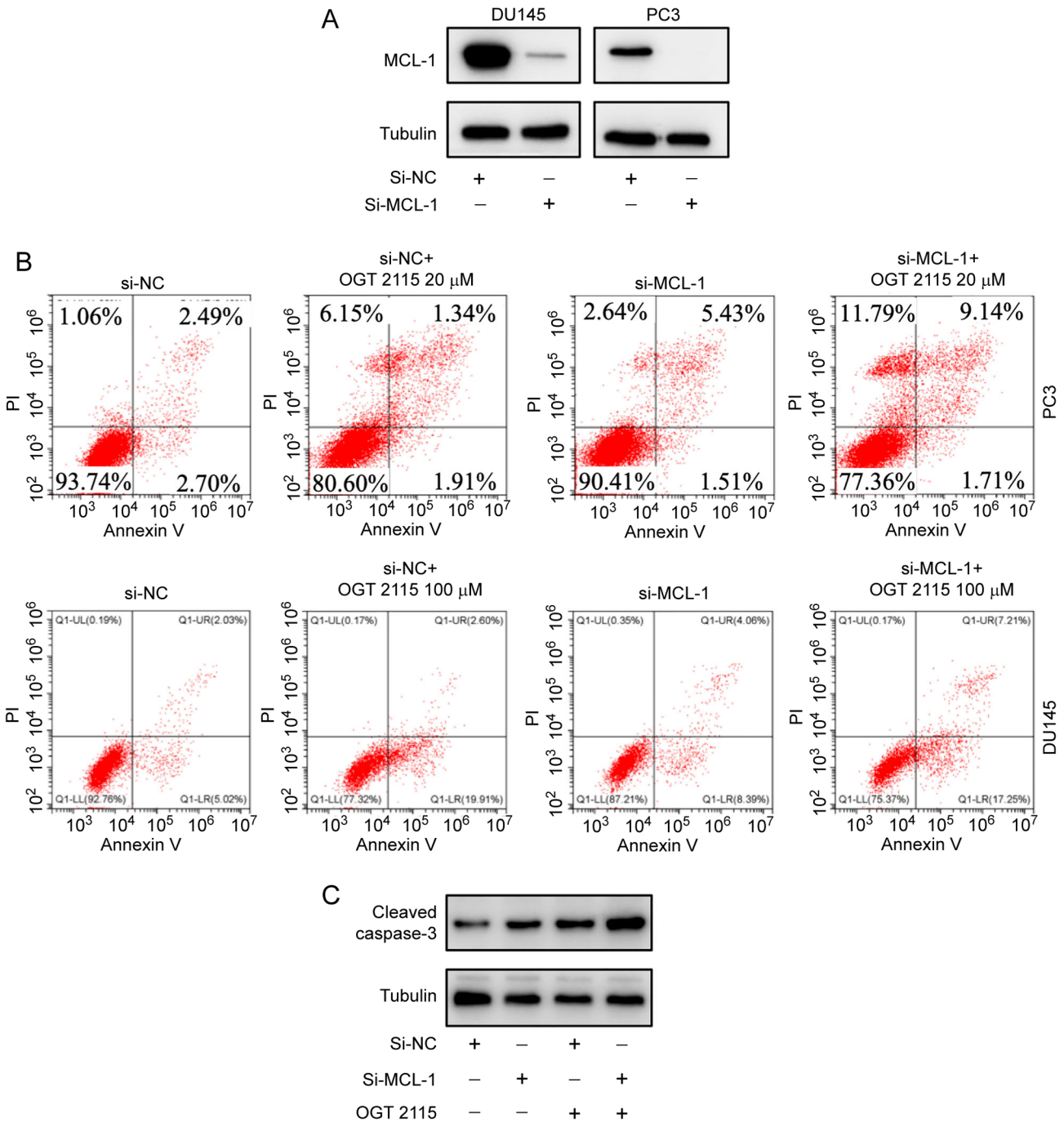

Figure 4. OGT 2115 induces prostate cancer cell apoptosis via the downregulation of MCL-1. (A) Protein expression levels of MCL-1 following si-MCL-1 transfection in PC-3 and DU-145 cells were determined via western blotting. Tubulin was used as the loading control. (B) Flow cytometry using annexin V (x-axis) and PI (y-axis) was conducted to determine the apoptosis rate in each experimental group, with or without si-MCL-1 transfection. (C) Protein expression levels of cleaved caspase-3 following OGT 2115 treatment with or without si-MCL-1 transfection in PC-3 cells were determined via western blotting. Tubulin was used as the loading control. MCL-1, myeloid cell leukemia-1; si, small interfering RNA; NC, negative control.

days 28 and 35 (Fig. 5A). The average tumor volume of the control group was 399.2 mm^3 and the largest was 738.1 mm^3, whereas the average tumor volume of the OGT 2115 group was 201.7 mm^3 and the largest was 365.5 mm^3. Furthermore, Ki67 immunohistochemical analysis was conducted to assess the proliferative ability of OGT 2115-treated prostate cancer cells. The results demonstrated a significant decrease in $Ki67^+$ cells in the OGT 2115 group compared with the control group (Fig. 5B). To further explore the effect of OGT 2115 on apoptosis in nude mice xenografts, TUNEL staining was performed. The results demonstrated that OGT 2115 treatment significantly increased the percentage of $TUNEL^+$ apoptotic cells in nude mice xenografts compared with the control (Fig. 5B). Furthermore, the HPSE and MCL-1 protein expression levels in the OGT 2115 group were markedly lower compared with the control group (Fig. 5C).

OGT 2115 decreases MCL-1 mRNA expression levels and facilitates MCL-1 protein degradation in prostate cancer cells. As OGT 2115 had been determined to reduce MCL-1

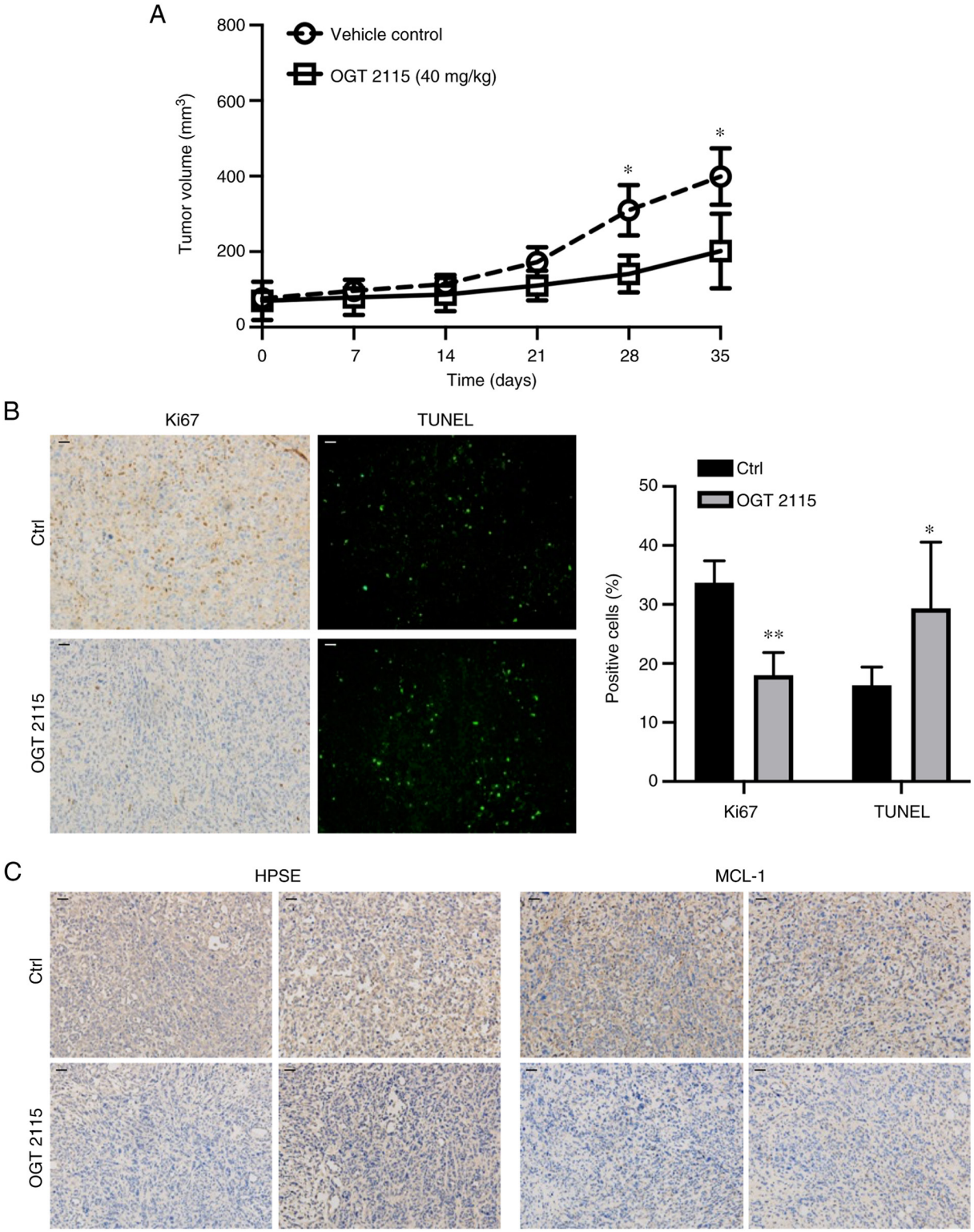

Figure 5. Effects of OGT 2115 on PC-3 cell xenograft growth and apoptosis in nude mice. (A) Effect of OGT 2115 (40 mg/kg/day via gavage for 5 weeks) on PC-3 cell xenograft growth (vehicle control, n=7; OGT 2115, n=6). (B) Effect of OGT 2115 (40 mg/kg/day via gavage for 5 weeks) on the percentage of Ki67$^+$ or TUNEL$^+$ PC-3 cells in xenograft tissues. (C) Effect of OGT 2115 (40 mg/kg/day via gavage for 5 weeks) on HPSE and MCL-1 protein expression levels in PC-3 cell xenograft tissues, determined using immunohistochemical staining analysis. Scale bar, 50 μm. *P<0.05 and **P<0.01 vs. Ctrl. HPSE, heparanase; MCL-1, myeloid cell leukemia-1; Ctrl, control.

protein expression levels in prostate cancer cells and xenografts, the underlying mechanism of OGT 2115-regulated MCL-1 expression was further investigated. RT-qPCR and western blotting were conducted to determine the MCL-1 mRNA and protein expression levels. In PC-3 cells, OGT 2115 treatment was administered at 0, 5, 10 and 20 μM for 24 h. In DU-145 cells, OGT 2115 treatment was administered at 0, 25, 50 and 100 μM for 24 h. The results of the RT-qPCR analysis demonstrated that OGT 2115 significantly reduced the MCL-1 mRNA expression levels

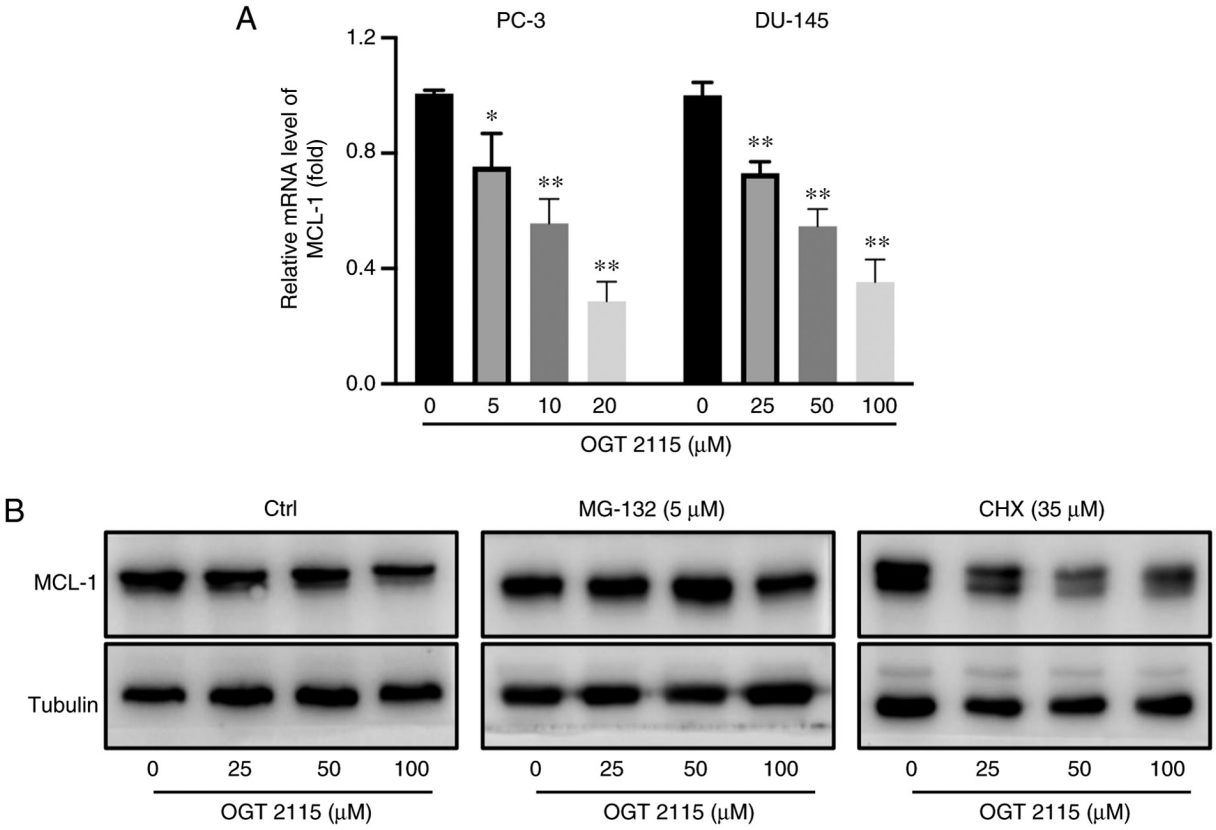

Figure 6. Effects of OGT 2115 on MCL-1 expression levels in prostate cancer cells. (A) Effect of OGT 2115 on MCL-1 mRNA expression levels in PC-3 and DU-145 cells, determined via reverse transcription-quantitative PCR. GAPDH was used as the internal reference gene. Data are presented as the fold change relative to the MCL-1 mRNA expression levels in the vehicle control (0 μM) cells. (B) Effect of OGT 2115, MG-132 (proteasome inhibitor; 10 μM; 1 h) and CHX (protein synthesis inhibitor; 100 μg/ml; 6 h) on MCL-1 protein expression levels, determined via western blotting. Tubulin was used as a loading control. All experiments were performed in triplicate. *P<0.05 and **P<0.01 vs. 0 μM. MCL-1, myeloid cell leukemia-1; CHX, cycloheximide; Ctrl, control.

in PC-3 and DU-145 cells compared with the 0 μM group, in a dose-dependent manner (Fig. 6A). Furthermore, the results of the western blotting analysis demonstrated that OGT 2115 markedly reduced the MCL-1 protein expression levels in prostate cancer cells in a dose-dependent manner (Fig. 6B). The protein synthesis inhibitor, CHX, was also administered to the OGT 2115 group for 6 h before detecting changes in MCL-1 protein expression. The results demonstrated that CHX did not affect the MCL-1 protein expression levels (Fig. 6B). Furthermore, the OGT 2115 group was treated with MG132, an inhibitor of proteasomal degradation. The results demonstrated that MG-132 markedly inhibited the decrease in MCL-1 protein expression levels caused by OGT 2115 treatment (Fig. 6B). It can therefore be concluded that OGT 2115 facilitates MCL-1 protein degradation instead of protein production in prostate cancer cells.

Discussion

In the present study, it was demonstrated that HPSE expression was higher in prostate cancer tissues compared with adjacent normal tissues. In addition, the HPSE inhibitor, OGT 2115, inhibited the viability of prostate cancer cells by inducing apoptosis. Further results demonstrated a correlation between HPSE and MCL-1 expression. Treatment with OGT 2115 decreased MCL-1 protein expression levels, and both RNA interference-mediated downregulation of MCL-1 and OGT 2115 treatment synergistically induced apoptosis in prostate cancer cells. Additional studies demonstrated that the proteasome inhibitor, MG-132, markedly inhibited the decrease in MCL-1 protein expression levels induced by OGT 2115. However, the protein synthesis inhibitor, CHX, did not affect the role of OGT 2115 in regulating MCL-1. The present study therefore demonstrated that the proapoptotic activity of OGT 2115 was achieved by downregulating MCL-1 expression, both transcriptionally and post-transcriptionally. However, the specific underlying mechanism of OGT 2115-induced degradation of MCL-1 requires further study.

HPSE is a β-glucuronidase that regulates the structure and function of HSPGs and remodels the cell surface and ECM by cleaving HS (25). A HSPG is formed by the polymerization of a core protein and one or more HS chains, in which the HS chain is the key active site (26). In normal human tissues, HPSE is mainly distributed in immune tissues, such as the placenta and lymphoid organs, but it is also widely distributed in tumors, particularly malignant tumor tissues, including prostate cancer (27). Typically, HPSE is associated with the tumor microenvironment (22). Previous studies have also demonstrated that HPSE increases the autophagy of tumor cells, which thereby increases their resistance to chemotherapy (28,29). HPSE upregulation promotes tumor growth, metastasis and angiogenesis (30), whereas the

downregulation of HPSE inhibits tumor proliferation and metastasis (31). Therefore, HPSE inhibitors may serve as anti-tumor therapeutics (32).

The molecular mechanism of OGT 2115 in promoting apoptosis in prostate cancer cells was explored in the present study. It was determined that the induction of apoptosis in prostate cancer cells by OGT 2115 was associated with MCL-1. The downregulation of MCL-1 expression levels in PC-3 and DU-145 cells promoted apoptosis following treatment with OGT 2115. MCL-1, a member of the Bcl-2 family of apoptosis-regulating genes, serves an antiapoptotic role via dimerizing BAK and Bax and binding to the Bcl-2 homology 3 (BH3) domain of the BH3-only protein (33). Furthermore, the MCL-1 protein is involved in the occurrence and development of tumors. It has been reported that amplification of the MCL-1 gene and an increase in MCL-1 protein expression levels are common in various types of tumor cells, such as breast, prostate and lung cancer cells (34-38). In addition, high MCL-1 expression levels lead to the resistance of tumor cells to chemotherapeutic drugs (39). Inhibiting the expression of MCL-1 or increasing its degradation promotes tumor cell apoptosis, which suggests that MCL-1 may be a potential therapeutic target (40). In the present study, immunohistochemistry demonstrated that the expression of MCL-1 in prostate cancer tissues was markedly higher than in adjacent normal tissues. In addition, western blotting demonstrated that OGT 2115 markedly reduced MCL-1 protein expression levels and markedly increased the protein expression levels of other apoptosis-related proteins, Bax and cleaved caspase-3, in prostate cancer cells. RT-qPCR demonstrated that OGT 2115 significantly downregulated the mRNA expression levels of MCL-1 in PC-3 and DU-145 cells. Furthermore, *in vivo* tumorigenic experiments in nude mice demonstrated that OGT 2115 significantly inhibited tumor proliferation and promoted apoptosis.

In conclusion, the results of the present study indicated that the HPSE inhibitor, OGT 2115, inhibited the viability of prostate cancer cells by decreasing MCL-1 levels both transcriptionally and post-transcriptionally. Furthermore, the present study provided a novel therapeutic approach for the treatment of prostate cancer. However, the specific underlying mechanism of OGT 2115-induced degradation of MCL-1 requires further study, and the antitumor effects of OGT 2115 should be validated in clinical trials.

Acknowledgements

We thank Mr. Bo-Ze Wang (Department of Pharmacology, Taizhou University, Taizhou, Zhejiang 318000, P.R. China) for their assistance with the flow cytometry assay.

Funding

This study was funded by Zhejiang Provincial Natural Science Foundation of China (grant nos. HDMY22H310084, LGF19H050004, LGD21H090002 and LGD20H310001).

Availability of data and materials

The datasets used and/or analyzed during the current study are available from the corresponding author on reasonable request.

Authors' contributions

XL, LLX and GC conceived and designed the study; XL and SCL confirmed the methods; XL, SCL, SJX, BJ, JC, HJL, HSL, SKZ and XFD helped with the acquisition of data (such as providing animals, acquiring and managing patients, and providing facilities) and performed the experiments; XL, GC, and LLX contributed to the analysis and interpretation of data (such as statistical analysis, biostatistics, and computational analysis). All authors read and approved the final manuscript. XL and GC confirm the authenticity of all the raw data.

Ethics approval and consent to participate

The studies involving human participants were reviewed and approved by The Medical Ethics Committee of Taizhou Central hospital (Taizhou, China; approval no. 2021-SC-076). The patients/participants provided written informed consent to participate in this study.

The animal study was reviewed and approved by The Medical Ethics Committee of Taizhou University College of Medicine (Taizhou, China; approval no. 2021-SX-015).

Patient consent for publication

Written informed consent for publication of clinical details and cancer tissues was obtained from the patients.

Competing interests

The authors declare that they have no competing interests.

References

1. Siegel RL, Miller KD, Fuchs HE and Jemal A: Cancer statistics, 2021. CA Cancer J Clin 71: 7-33, 2021.
2. Chen W, Zheng R, Baade PD, Zhang S, Zeng H, Bray F, Jemal A, Yu XQ and He J: Cancer statistics in China, 2015. CA Cancer J Clin 66: 115-132, 2016.
3. Perlmutter MA and Lepor H: Androgen deprivation therapy in the treatment of advanced prostate cancer. Rev Urol 9 (Suppl 1): S3-S8, 2007.
4. Limberger T, Schlederer M, Trachtová K, Garces de Los Fayos Alonso I, Yang J, Högler S, Sternberg C, Bystry V, Oppelt J, Tichý B, *et al*: KMT2C methyltransferase domain regulated INK4A expression suppresses prostate cancer metastasis. Mol Cancer 21: 89, 2022.
5. Smith MR, Saad F, Coleman R, Shore N, Fizazi K, Tombal B, Miller K, Sieber P, Karsh L, Damião R, *et al*: Denosumab and bone-metastasis-free survival in men with castration-resistant prostate cancer: Results of a phase 3, randomised, placebo-controlled trial. Lancet 379: 39-46, 2012.
6. Vlodavsky I, Ilan N and Sanderson RD: Forty years of basic and translational heparanase research. Adv Exp Med Biol 1221: 3-59, 2020.
7. Reynolds MR, Singh I, Azad TD, Holmes BB, Verghese PB, Dietrich HH, Diamond M, Bu G, Han BH and Zipfel GJ: Heparan sulfate proteoglycans mediate Aβ-induced oxidative stress and hypercontractility in cultured vascular smooth muscle cells. Mol Neurodegener 11: 9, 2016.
8. Koganti R, Suryawanshi R and Shukla D: Heparanase, cell signaling, and viral infections. Cell Mol Life Sci 77: 5059-5077, 2020.
9. Cohen-Kaplan V, Jrbashyan J, Yanir Y, Naroditsky I, Ben-Izhak O, Ilan N, Doweck I and Vlodavsky I: Heparanase induces signal transducer and activator of transcription (STAT) protein phosphorylation: preclinical and clinical significance in head and neck cancer. J Biol Chem 287: 6668-6678, 2012.

10. Mahtouk K, Hose D, Raynaud P, Hundemer M, Jourdan M, Jourdan E, Pantesco V, Baudard M, De Vos J, Larroque M, *et al*: Heparanase influences expression and shedding of syndecan-1, and its expression by the bone marrow environment is a bad prognostic factor in multiple myeloma. Blood 109: 4914-4923, 2007.
11. Fletcher S: MCL-1 inhibitors-where are we now (2019)? Expert Opin Ther Pat 29: 909-919, 2019.
12. Abdul Rahman SF, Azlan A, Lo KW, Azzam G and Mohana-Kumaran N: Dual inhibition of anti-apoptotic proteins BCL-XL and MCL-1 enhances cytotoxicity of Nasopharyngeal carcinoma cells. Discov Oncol 13: 9, 2022.
13. Wang B, Ni Z, Dai X, Qin L, Li X, Xu L, Lian J and He F: The Bcl-2/xL inhibitor ABT-263 increases the stability of Mcl-1 mRNA and protein in hepatocellular carcinoma cells. Mol Cancer 13: 98, 2014.
14. Carné Trécesson S, Souazé F, Basseville A, Bernard AC, Pécot J, Lopez J, Bessou M, Sarosiek KA, Letai A, Barillé-Nion S, *et al*: BCL-X(L) directly modulates RAS signalling to favour cancer cell stemness. Nat Commun 8: 1123, 2017.
15. Wei AH, Roberts AW, Spencer A, Rosenberg AS, Siegel D, Walter RB, Caenepeel S, Hughes P, McIver Z, Mezzi K, *et al*: Targeting MCL-1 in hematologic malignancies: Rationale and progress. Blood Rev 44: 100672, 2020.
16. Yancey D, Nelson KC, Baiz D, Hassan S, Flores A, Pullikuth A, Karpova Y, Axanova L, Moore V, Sui G and Kulik G: BAD dephosphorylation and decreased expression of MCL-1 induce rapid apoptosis in prostate cancer cells. PLoS One 8: e74561, 2013.
17. Cancer Genome Atlas Research Network. The molecular taxonomy of primary prostate cancer. Cell 4: 1011-1025, 2015.
18. Chandrashekar DS, Karthikeyan SK, Korla PK, Patel H, Shovon AR, Athar M, Netto GJ, Qin ZS, Kumar S, Manne U, *et al*: UALCAN: An update to the integrated cancer data analysis platform. Neoplasia 25: 18-27, 2022.
19. Chandrashekar DS, Bashel B, Balasubramanya SAH, Creighton CJ, Rodriguez IP, Chakravarthi BVSK and Varambally S: UALCAN: A portal for facilitating tumor subgroup gene expression and survival analyses. Neoplasia 8: 649-658, 2017.
20. Epstein JI, Egevad L, Amin MB, Delahunt B, Srigley JR, Humphrey PA and Grading Committee: The 2014 international society of urological pathology (ISUP) consensus conference on gleason grading of prostatic carcinoma: Definition of grading patterns and proposal for a new grading system. Am J Surg Pathol 2: 244-252, 2016.
21. Livak KJ and Schmittgen TD: Analysis of relative gene expression data using real-time quantitative PCR and the 2(-Delta Delta C(T)) method. Methods 25: 402-408, 2001.
22. MacArthur Clark JA and Sun D: Guidelines for the ethical review of laboratory animal welfare people's republic of China national standard GB/T 35892-2018 (Issued 6 February 2018 Effective from 1 September 2018). Animal Model Exp Med 3: 103-113, 2020.
23. Jiao W, Chen Y, Song H, Li D, Mei H, Yang F, Fang E, Wang X, Huang K, Zheng L and Tong Q: HPSE enhancer RNA promotes cancer progression through driving chromatin looping and regulating hnRNPU/p300/EGR1/HPSE axis. Oncogene 20: 2728-2745, 2018.
24. Wang H, Guo M, Wei H and Chen Y: Targeting MCL-1 in cancer: current status and perspectives. J Hematol Oncol 1: 67, 2021.
25. Sanderson RD, Elkin M, Rapraeger AC, Ilan N and Vlodavsky I: Heparanase regulation of cancer, autophagy and inflammation: New mechanisms and targets for therapy. FEBS J 284: 42-55, 2017.
26. Tumova S, Woods A and Couchman JR: Heparan sulfate proteoglycans on the cell surface: versatile coordinators of cellular functions. Int J Biochem Cell Biol 32: 269-288, 2000.
27. Zhou Y, Song B, Qin WJ, Zhang G, Zhang R, Luan Q, Pan TJ, Yang AG and Wang H: Heparanase promotes bone destruction and invasiveness in prostate cancer. Cancer Lett 268: 252-259, 2008.
28. Li QW, Zhang GL, Hao CX, Ma YF, Sun X, Zhang Y, Cao KX, Li BX, Yang GW and Wang XM: SANT, a novel Chinese herbal monomer combination, decreasing tumor growth and angiogenesis via modulating autophagy in heparanase overexpressed triple-negative breast cancer. J Ethnopharmacol 266: 113430, 2021.
29. Shteingauz A, Boyango I, Naroditsky I, Hammond E, Gruber M, Doweck I, Ilan N and Vlodavsky I: Heparanase enhances tumor growth and chemoresistance by promoting autophagy. Cancer Res 75: 3946-3957, 2015.
30. Tatsumi Y, Miyake M, Shimada K, Fujii T, Hori S, Morizawa Y, Nakai Y, Anai S, Tanaka N, Konishi N and Fujimoto K: Inhibition of heparanase expression results in suppression of invasion, migration and adhesion abilities of bladder cancer cells. Int J Mol Sci 21: 3789, 2020.
31. Vlodavsky I, Beckhove P, Lerner I, Pisano C, Meirovitz A, Ilan N and Elkin M: Significance of heparanase in cancer and inflammation. Cancer Microenviron 5: 115-132, 2012.
32. Masola V, Zaza G, Onisto M, Lupo A and Gambaro G: Impact of heparanase on renal fibrosis. J Transl Med 13: 181, 2015.
33. Morciano G, Giorgi C, Balestra D, Marchi S, Perrone D, Pinotti M and Pinton P: Mcl-1 involvement in mitochondrial dynamics is associated with apoptotic cell death. Mol Biol Cell 27: 20-34, 2016.
34. Luo W, Nagaria TS, Sun H, Ma J, Lombardo JL, Bassett R, Cao AC and Tan D: Expression and potential prognostic value of SOX9, MCL-1 and SPOCK1 in gastric adenocarcinoma. Pathol Oncol Res 28: 1610293, 2022.
35. Vela L and Marzo I: Bcl-2 family of proteins as drug targets for cancer chemotherapy: The long way of BH3 mimetics from bench to bedside. Curr Opin Pharmacol 23: 74-81, 2015.
36. Bashari MH, Fan F, Vallet S, Sattler M, Arn M, Luckner-Minden C, Schulze-Bergkamen H, Zörnig I, Marme F, Schneeweiss A, *et al*: Mcl-1 confers protection of Her2-positive breast cancer cells to hypoxia: Therapeutic implications. Breast Cancer Res 18: 26, 2016.
37. Omari S, Waters M, Naranian T, Kim K, Perumalsamy AL, Chi M, Greenblatt E, Moley KH, Opferman JT and Jurisicova A: Mcl-1 is a key regulator of the ovarian reserve. Cell Death Dis 6: e1755, 2015.
38. Ma J, Zhao Z, Wu K, Xu Z and Liu K: MCL-1 is the key target of adjuvant chemotherapy to reverse the cisplatin-resistance in NSCLC. Gene 587: 147-154, 2016.
39. Xiang W, Yang CY and Bai L: MCL-1 inhibition in cancer treatment. Onco Targets Ther 11: 7301-7314, 2018.
40. Leverson JD, Zhang H, Chen J, Tahir SK, Phillips DC, Xue J, Nimmer P, Jin S, Smith M, Xiao Y, *et al*: Potent and selective small-molecule MCL-1 inhibitors demonstrate on-target cancer cell killing activity as single agents and in combination with ABT-263 (navitoclax). Cell Death Dis 6: e1590, 2015.